LETTER

doi:10.1038/nature09669

Identification of adult nephron progenitors capable of kidney regeneration in zebrafish

Cuong Q. Diep[1,2], Dongdong Ma[2,3], Rahul C. Deo[1,2], Teresa M. Holm[1,2], Richard W. Naylor[1,2], Natasha Arora[1], Rebecca A. Wingert[1,2,4], Frank Bollig[5], Gordana Djordjevic[1], Benjamin Lichman[1], Hao Zhu[6], Takanori Ikenaga[7], Fumihito Ono[7], Christoph Englert[5,8], Chad A. Cowan[1,2,4,9], Neil A. Hukriede[10], Robert I. Handin[2,3,4] & Alan J. Davidson[1,2,4]†

Loss of kidney function underlies many renal diseases[1]. Mammals can partly repair their nephrons (the functional units of the kidney), but cannot form new ones[2,3]. By contrast, fish add nephrons throughout their lifespan and regenerate nephrons *de novo* after injury[4,5], providing a model for understanding how mammalian renal regeneration may be therapeutically activated. Here we trace the source of new nephrons in the adult zebrafish to small cellular aggregates containing nephron progenitors. Transplantation of single aggregates comprising 10–30 cells is sufficient to engraft adults and generate multiple nephrons. Serial transplantation experiments to test self-renewal revealed that nephron progenitors are long-lived and possess significant replicative potential, consistent with stem-cell activity. Transplantation of mixed nephron progenitors tagged with either green or red fluorescent proteins yielded some mosaic nephrons, indicating that multiple nephron progenitors contribute to a single nephron. Consistent with this, live imaging of nephron formation in transparent larvae showed that nephrogenic aggregates form by the coalescence of multiple cells and then differentiate into nephrons. Taken together, these data demonstrate that the zebrafish kidney probably contains self-renewing nephron stem/progenitor cells. The identification of these cells paves the way to isolating or engineering the equivalent cells in mammals and developing novel renal regenerative therapies.

Zebrafish nephrons in the adult kidney are similar to those found in the embryonic kidney[6], except that they are highly branched and drained by two central collecting ducts (Fig. 1a and Supplementary Fig. 2a–j). We confirmed that zebrafish nephron number increases with age (Fig. 1b), similar to other fish[4,5]. To identify the source of new nephrons in adult zebrafish, we first characterized the effects of gentamicin injection, an established nephrotoxin[7]. Intraperitoneal injection of gentamicin induced nephron damage, downregulated the proximal tubule marker *slc20a1a* and resulted in a failure to take up filtered 40 kDa fluorescent dextran[8] by 1 day post-injection (Fig. 1c–f, $n = 6/6$; Fig. 1j–k, $n = 8/8$; Supplementary Fig. 2k–p). Around 4 days post-injection, partial restoration in nephron function was observed, suggesting some nephrons recovered from the injury (Fig. 1g, l, arrow). At this stage we also detected small, but appropriately proportioned, nephrons that were dextran-positive, proliferating and basophilic, which are characteristic features of immature nephrons[7] (approximately 15 per kidney; Fig. 1i, l inset, n). By 15 days post-injection the damaged nephrons had recovered to near-normal levels, although immature nephrons could still be detected (Fig. 1h, m, arrow).

If the adult kidney contains nephron progenitors responsible for the formation of new nephrons, then these cells might be amenable to transplantation. To test this, we developed a transplantation assay (Fig. 2a and Supplementary Fig. 3a–k) in which recipient fish were immunocompromised by radiation to prevent graft rejection[9] and then injected with gentamicin. Unpurified whole-kidney marrow cells (WKM), mostly comprising non-tubular interstitial cells[9], were prepared from Tg(*cdh17:EGFP*)[10] or Tg(*cdh17:mCherry*) donors that express fluorescent reporters in the distal nephron. Injection of approximately 5×10^5 of these cells resulted in donor-derived nephrons in 100% of the recipients ($n = 6$) by 18 days post-transplantation (d.p.t.), with an average of 24 donor-derived nephrons (Fig. 2b, arrow, inset). Donor nephron number increased with time, reaching an average of 70 nephrons by 59 d.p.t. (Fig. 2c) and greatly expanded the head kidney on the injected side (Fig. 2d, arrow). At these later time points, we also found donor-derived nephrons in locations distant from the site of injection, which suggests that the transplanted cells are migratory (Supplementary Fig. 3l, arrowheads).

To regenerate damaged tissue successfully, newly created structures must incorporate into existing tissue. To determine whether the donor-derived nephrons were capable of blood filtration, we injected 40 kDa fluorescent dextran into transplant recipients that had received WKM from Tg(*cdh17:mCherry*) donor fish and dissected out individual nephrons. All of the donor-derived nephrons examined ($n = 5$) were dextran-positive (Fig. 2e), indicating that they had integrated into the recipient's blood supply. These results show that nephron progenitors are present in the adult kidney and that after transplantation they are capable of forming new functional nephrons within the host's renal tissue.

Cell transplantation experiments can be confounded by the fusion of donor and recipient cells. To address this, we injected WKM from Tg(*cdh17:mCherry*) donors into Tg(*cdh17:EGFP*) recipients. If fusion occurred, we would expect to find nephrons positive for both mCherry and enhanced green fluorescent protein (EGFP). An analysis of engrafted recipients ($n = 6$) revealed that all of the mCherry-positive nephrons were EGFP-negative, providing evidence that they had not formed by cell–cell fusion. In addition, we identified the connection of the donor-derived nephrons with the host's renal tubules, providing further evidence that the engrafted nephrons had successfully integrated into the recipient's renal system (Fig. 2f).

Lineage labelling studies in the developing mouse kidney have revealed that multiple *Six2*$^+$ cap mesenchyme cells, the source of nephron progenitors, contribute to a single nephron[11]. To explore this in zebrafish, we transplanted a 1:1 mix of Tg(*cdh17:EGFP*) and Tg(*cdh17:mCherry*) WKM cells into conditioned recipients. Mosaic nephrons containing both EGFP-positive and mCherry-positive cells were found in 27% of the engrafted fish ($n = 15$; Fig. 2g), although the remaining nephrons were either all EGFP-positive or all mCherry-positive. Thus multiple nephron progenitors can contribute to an individual nephron.

[1]Center for Regenerative Medicine, Massachusetts General Hospital, Boston, Massachusetts 02114, USA. [2]Harvard Medical School, Boston, Massachusetts 02115, USA. [3]Hematology Division, Brigham and Women's Hospital, Boston, Massachusetts 02115, USA. [4]Harvard Stem Cell Institute, Cambridge, Massachusetts 02138, USA. [5]Leibniz Institute for Age Research, Fritz Lipmann Institute, Jena D-07745, Germany. [6]Dana-Farber Cancer Institute, Boston, Massachusetts 02115, USA. [7]Section on Model Synaptic Systems, Laboratory of Molecular Physiology, National Institutes of Health/National Institute on Alcohol Abuse and Alcoholism, Bethesda, Maryland 20892, USA. [8]Friedrich-Schiller-University, Jena D-07743, Germany. [9]Department of Stem Cell and Regenerative Biology, Harvard University, Cambridge, Massachusetts 02138, USA. [10]Department of Developmental Biology, University of Pittsburgh, School of Medicine, Pittsburgh, Pennsylvania 15260, USA. †Present address: Department of Molecular Medicine and Pathology, School of Medical Sciences, The University of Auckland, Auckland 1142, New Zealand.

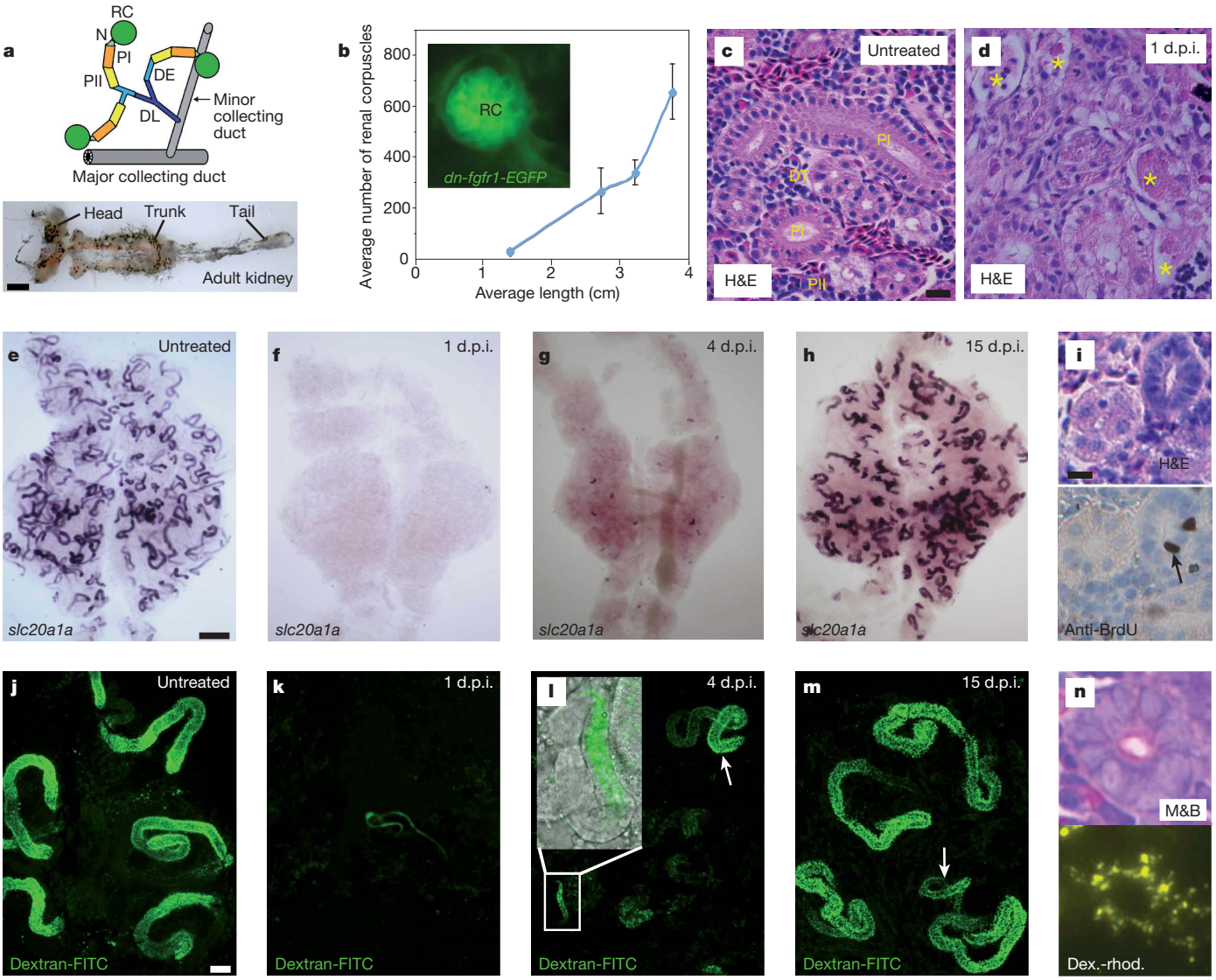

Figure 1 | The adult zebrafish kidney undergoes nephrogenesis throughout life and after injury. **a**, Zebrafish kidney and nephron model (scale bar, 1 mm). **b**, Graph showing average number of renal corpuscles (RC) relative to body length (inset shows an RC labelled with *dn-fgfr1-EGFP*[18]) (error bar, one standard deviation; $n = 3$ fish per time point). RC, renal corpuscle; N, neck; PI, proximal tubule I; PII, proximal tubule II; DE, distal early; DL, distal late. **c**, **d**, Kidney sections showing gentamicin-damaged nephrons (asterisks; scale bar, 10 μm). H&E, haematoxylin and eosin; d.p.i., days post-injection; DT, distal tubule. **e–h**, Expression of *slc20a1a* in gentamicin-damaged kidneys (scale bar, 0.5 mm). **i**, Immature nephron with dividing cells (arrow) (scale bar, 10 μm). **j–m**, Uptake of 40 kDa fluorescein isothiocyanate (FITC)-conjugated dextran by gentamicin-damaged kidneys (inset in **l** shows an immature nephron; arrow in **l** marks a positive nephron; arrow in **m** indicates an immature nephron; scale bar, 30 μm). **n**, Serial sections showing that immature basophilic nephrons take up 40 kDa dextran-rhodamine. M&B, methylene blue and basic fuchsin.

Mammalian *Six2*$^+$ cap mesenchyme cells are also characterized by their stem-cell-like self-renewal properties[11]. Serial transplantation is used to distinguish haematopoietic stem cells from progenitors[12]. We investigated whether we could obtain donor-derived nephrons after serial transplantation of WKM from engrafted recipients (Fig. 2h). We transplanted WKM from primary fish containing 2–89 *cdh17:EGFP*$^+$ donor-derived nephrons and achieved a 48% ($n = 21$) engraftment rate in secondary fish, with the number of donor-derived nephrons ranging from 1 to 53 by 41 d.p.t. The WKM from one of these secondary fish, containing 53 engrafted nephrons, was transplanted again and successfully engrafted a third time, giving rise to 12 donor-derived nephrons in the tertiary recipient at 35 d.p.t. (a total of 135 days from primary to tertiary fish; Fig. 2i–k). These results demonstrate that nephron progenitors possess significant proliferative potential, consistent with self-renewing capabilities.

We next sought to identify the cells responsible for nephron progenitor activity. We noted that approximately 0.1% of the WKM from Tg(*cdh17:EGFP*) fish is EGFP-positive (Supplementary Fig. 4a). To test whether *cdh17:EGFP*$^+$ cells could contribute to new nephrons, we sorted and transplanted this fraction (approximately 5,000 cells per fish) but failed to observe engraftment ($n = 0/7$). We subsequently explored other markers of nephron progenitors. In mammals, nephrogenesis initiates with the formation of 'pre-tubular aggregates' that undergo a mesenchymal-to-epithelial transition into renal vesicles[13]. These structures express several transcription factors including *Lhx1/Lim1* (ref. 14) and *Wt1* (ref. 15). We therefore examined the Tg(*lhx1a:EGFP*)[16] and Tg(*wt1b:mCherry*) transgenic lines to determine whether these reporters mark nephron progenitors. Kidneys from untreated Tg(*lhx1a:EGFP*) adults were found to contain three distinctive EGFP-positive cell populations: (1) single cells with a mesenchymal morphology (Fig. 3a) that make up approximately 0.02% of the WKM (Supplementary Fig. 4b), (2) homogeneous aggregates of *lhx1a:EGFP*$^+$ mesenchymal cells ranging from a few to approximately 30 cells (Fig. 3b, c and Supplementary Fig. 4i) (approximately 100 aggregates

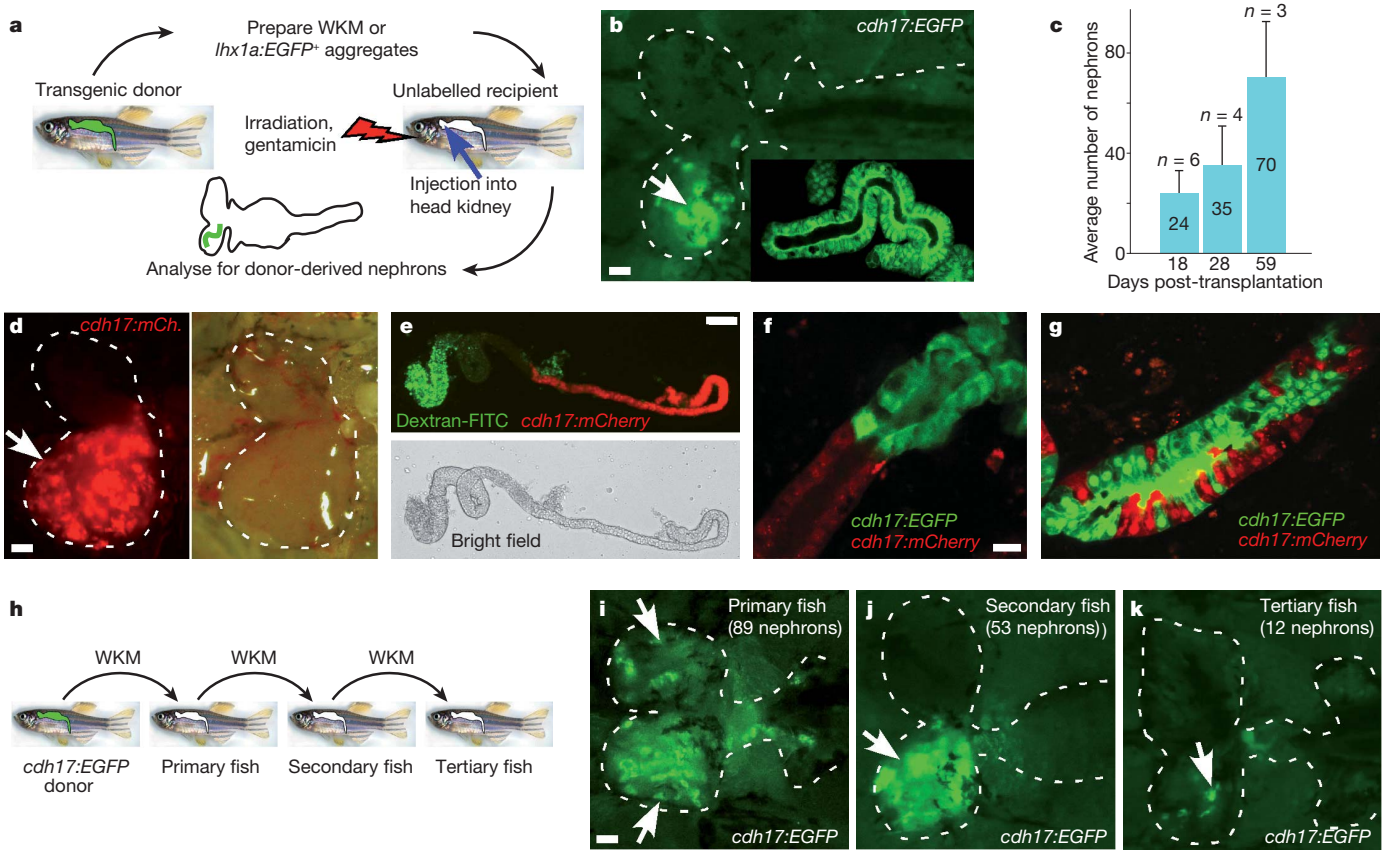

Figure 2 | The adult zebrafish kidney contains transplantable progenitors that form functional nephrons. **a**, Overview of the transplantation assay. **b**, A primary transplanted fish at 18 d.p.t. with *cdh17:EGFP*$^+$ donor-derived nephrons (arrow; inset, higher magnification view; scale bar, 0.5 mm). **c**, Average number of donor-derived nephrons over time (error bar, one standard deviation; *n*, total fish per time point). **d**, Head kidney of a recipient at 34 d.p.t. showing expansion of renal tissue caused by *cdh17:mCherry*$^+$ donor-derived nephrons (arrow; scale bar, 0.5 mm). **e**, A *cdh17:mCherry*$^+$ donor-derived nephron showing functional uptake of 40 kDa FITC-conjugated dextran (scale bar, 30 μm). **f**, Connection of donor-derived nephrons (*cdh17:mCherry*$^+$) with the *cdh17:EGFP*$^+$ recipient's renal system (scale bar, 10 μm). **g**, A mosaic nephron arising from the co-injection of a mixture of *cdh17:EGFP*- and *cdh17:mCherry*-labelled nephron progenitors. **h**, Overview of the serial transplantation assay. **i**–**k**, Donor-derived nephrons (*cdh17:EGFP*$^+$, arrows) in primary-, secondary- and tertiary-engrafted recipients (scale bar, 0.5 mm).

per kidney) and (3) renal vesicle-like bodies (0–2 per kidney; Fig. 3d). The last two populations were highly reminiscent of pre-tubular aggregates and renal vesicles in mammals.

An examination of Tg(*lhx1a:EGFP;wt1b:mCherry*) double transgenic kidneys revealed that only the large aggregates and renal vesicles, but not the other *lhx1a:EGFP*$^+$ populations, were *wt1b:mCherry*$^+$ (Fig. 3d). We hypothesized that the *lhx1a:EGFP*$^+$/*wt1b:mCherry*$^+$ renal vesicle-like bodies, which were rare in untreated kidneys, constitute primitive nephrons. Consistent with this, gentamicin treatment greatly induced the formation of *lhx1a:EGFP*$^+$/*wt1b:mCherry*$^+$ double-positive cells (data not shown) and activated the endogenous expression of the early-acting renal genes *pax2a*, *fgf8a*, *wt1a* and *wt1b* in similar structures (Fig. 3e–j and Supplementary Fig. 4c–h). We failed to detect the expression of mature nephron markers in structures resembling either *lhx1a:EGFP*$^+$ aggregates or *wt1b*$^+$ renal vesicles (Supplementary Fig. 5a–c and Supplementary Table 1). Similarly, quantitative PCR analysis of purified *lhx1a:EGFP*$^+$ and *cdh17:EGFP*$^+$ cells showed that *lhx1a:EGFP*$^+$ cells express considerably lower levels of mature nephron markers than *cdh17:EGFP*$^+$ cells (Supplementary Fig. 5d). These findings suggest that *lhx1a:EGFP* labels nephron progenitors and *lhx1a:EGFP/wt1b:mCherry* labels early-stage nephrons.

To clarify the lineage relationships between *lhx1a:EGFP*$^+$ and *lhx1a:EGFP*$^+$/*wt1b:mCherry*$^+$ cells, we took advantage of the optical transparency of larval fish to visualize nephrogenesis *in vivo*. By observing Tg(*cdh17:EGFP*) larvae as well as using wholemount *in situ* hybridization, we found that adult kidney formation initiates at the 5.2-mm stage (approximately 13 days post-fertilization). The first nephron appears consistently on the embryonic (pronephric) renal tubules just posterior to the swim bladder (Supplementary Fig. 6a–e and data not shown). *lhx1a:EGFP*$^+$ cells appeared before this, at the 4-mm stage (approximately 10 days post-fertilization) (Fig. 4a, arrow, inset), rapidly migrated along the pronephric tubules (Fig. 4b, arrows), and formed into aggregates (Fig. 4b, arrowheads). An *in vivo* time course of Tg(*lhx1a:EGFP;cdh17:mCherry*) and Tg(*lhx1a:EGFP;wt1b:mCherry*) larvae showed that the *lhx1a:EGFP*$^+$ aggregates arose from the coalescence of three or four *lhx1a:EGFP*$^+$ cells that expanded to form a renal vesicle and activated expression of *wt1b:mCherry* (Fig. 4d and Supplementary Fig. 6f). Similar time courses of Tg(*lhx1a:EGFP;cdh17:mCherry)* and Tg(*wt1b:EGFP;pax8:DsRed*) larvae demonstrated that the renal vesicle elongated into a *cdh17*$^+$ nephron, with *lhx1a*$^+$ cells becoming restricted to the point of fusion with the pronephric tubules, *pax8* initiating in the distal tubule and *wt1b* labelling the glomerulus and proximal tubule (Fig. 4e and Supplementary Fig. 6g). To demonstrate a requirement of *lhx1a:EGFP*$^+$ cells for nephrogenesis, we ablated single *lhx1a:EGFP*$^+$ aggregates with a laser (Fig. 4c, arrow), resulting in aborted nephrogenesis in the targeted region without affecting neighbouring nephrons (Fig. 4c, arrowhead) ($n = 2/2$).

Next we tested whether *lhx1a:EGFP*$^+$ cells had nephron-forming activity. Transplantation of single *lhx1a:EGFP*$^+$ cells failed to engraft conditioned recipients. However, transplantation of individual *lhx1a:EGFP*$^+$ aggregates resulted in successful engraftment in 33% ($n = 15$) of transplanted fish (Fig. 4f, g). In one case, a single aggregate contributed to 16 nephrons, 27 aggregates and numerous individual cells (Supplementary Fig. 7a–c), consistent with *lhx1a:EGFP*$^+$ cells

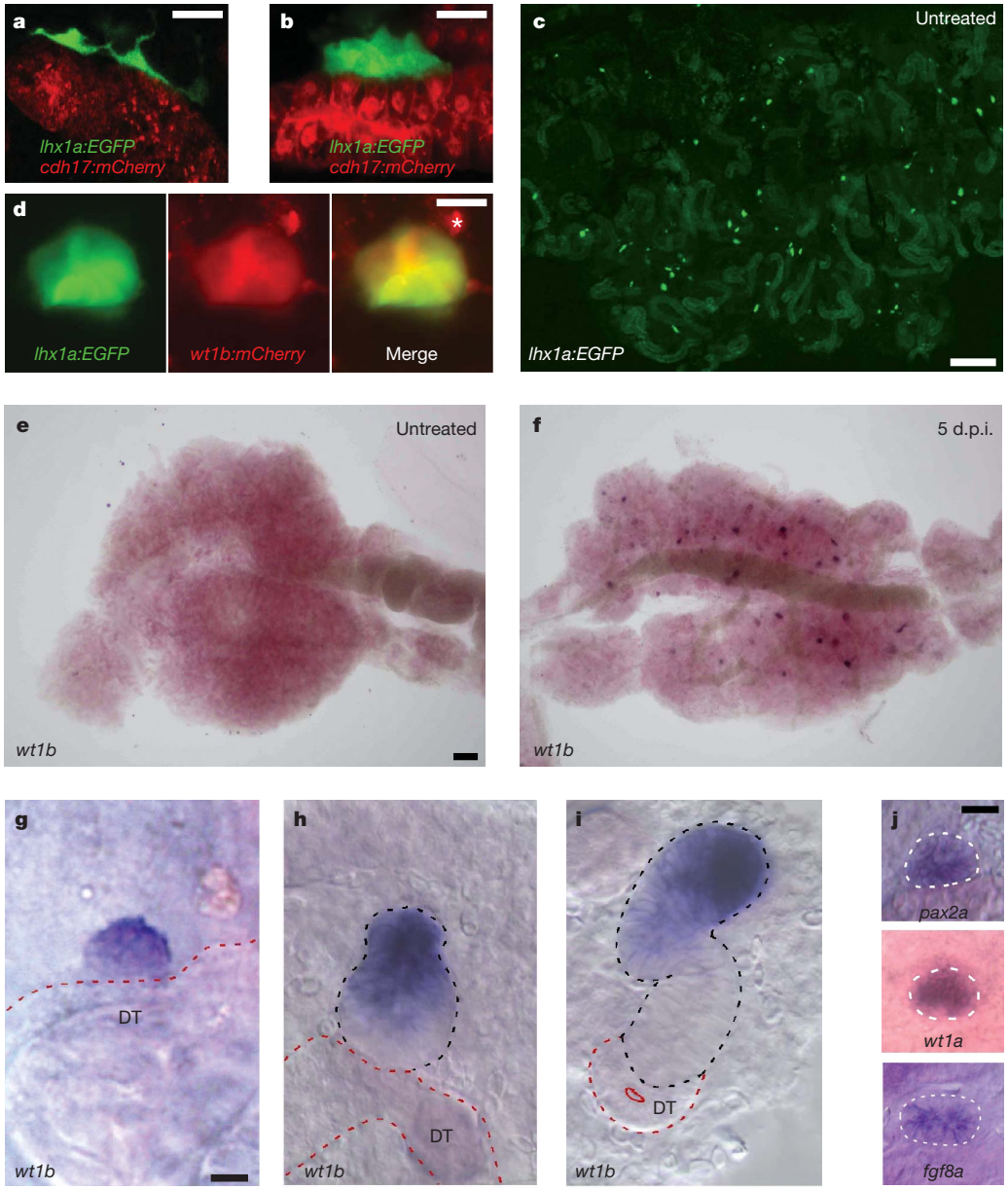

Figure 3 | Expression of *lhx1a:EGFP* and other renal factors in the adult kidney. **a**, Single mesenchymal cells labelled with *lhx1a:EGFP* (scale bar, 10 μm). **b**, Small aggregates labelled with *lhx1a:EGFP* (scale bar, 10 μm). **c**, An untreated kidney showing *lhx1a:EGFP*$^+$ aggregates in a portion of the trunk region; scale bar, 0.5 mm). **d**, Co-expression of *wt1b:mCherry* and *lhx1a:EGFP* in large aggregates (asterisk, autofluorescence; scale bar, 10 μm). **e**, **f**, Expression of *wt1b* in untreated and gentamicin-damaged kidneys (scale bar, 0.5 mm). **g**–**i**, Expression of *wt1b* in a large aggregate (**g**), a comma-shaped body (**h**) and an immature nephron (**i**) in gentamicin-damaged kidneys (scale bar, 10 μm). **j**, Expression of *pax2a*, *wt1a* and *fgf8a* in large aggregates or renal vesicles in gentamicin-damaged kidneys (scale bar, 10 μm).

having extensive proliferative and self-renewing capabilities. Transplantation of *lhx1a:EGFP*$^+$/*wt1b:mCherry*$^+$ renal vesicles failed to engraft ($n = 0/10$), suggesting that nephron-forming potential is restricted to *lhx1a:EGFP*$^+$ aggregates. These findings demonstrate that *lhx1a:EGFP*$^+$ aggregates contain nephron progenitors and support our observation that multiple nephron progenitors are needed to form a nephron.

To determine how similar *lhx1a:EGFP*$^+$ cells are to *Six2*$^+$ mouse cap mesenchyme cells, we conducted a microarray analysis, comparing the genes upregulated in *lhx1a:EGFP*$^+$ cells (relative to *cdh17:EGFP*$^+$ epithelial cells) with those upregulated in mouse *Six2*$^+$ cells (relative to mouse proximal tubule epithelial cells). At a global level, the respective gene sets that are upregulated in *lhx1a:EGFP*$^+$ cells and *Six2*$^+$ cells are not significantly similar (Supplementary Tables 2–4 and Supplementary Fig. 8a). However, there is conservation of several factors implicated in renal development and/or stem-cell self-renewal. Notably, orthologues of *Six2* (*six2a*) and *Wt1* (*wt1a*), which are essential for cap mesenchyme maintenance, are upregulated both in *lhx1a:EGFP*$^+$ cells and in *Six2*$^+$ cells. Quantitative PCR confirmed that *six2a* and *wt1a* are expressed over 15-fold higher in *lhx1a:EGFP*$^+$ cells than *cdh17:EGFP*$^+$ cells (Supplementary Fig. 8b). Several other potentially important regulators were also identified in the comparison, including *Meis2*, *Ezh2* and *Tcf3*, which are implicated in Wnt signalling and/or stem-cell function (Supplementary Table 4). These results suggest that, despite having distinct molecular identities, zebrafish *lhx1a:EGFP*$^+$ cells and *Six2*$^+$ cells share a core set of regulatory genes that may be important for conferring renal stem/progenitor cell potential.

In conclusion, we have identified an adult population of nephron progenitors that reside in small aggregates throughout the zebrafish kidney. These cells are uniquely defined by their ability to form new functional nephrons during zebrafish growth, injury and after transplantation. Nephron progenitors can be serially transplanted, consistent

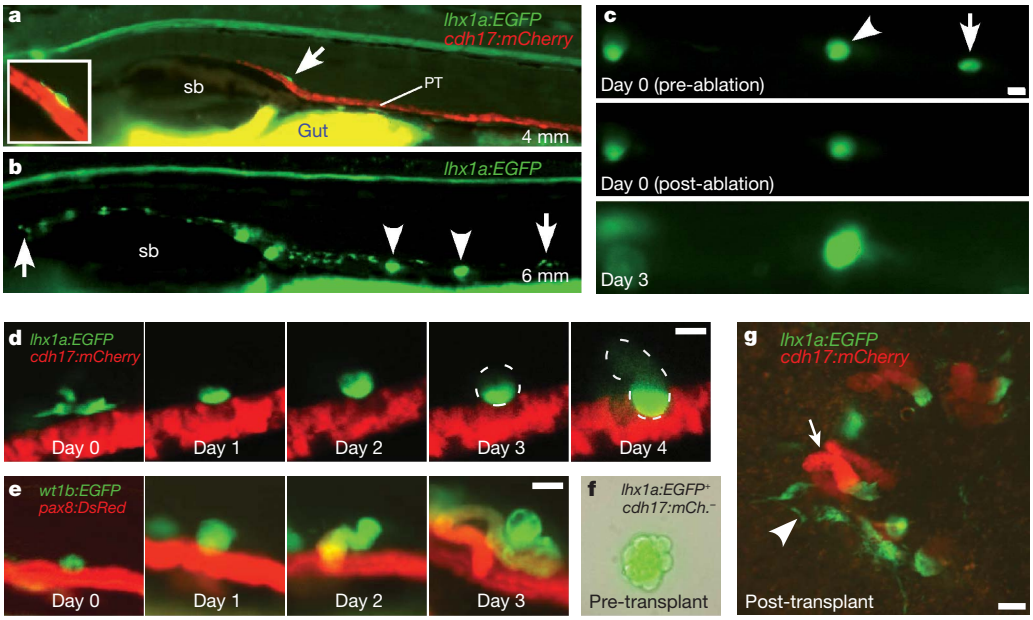

Figure 4 | *lhx1a:EGFP*$^+$ cells form nephrons during adult kidney development and after transplantation. **a**, Lateral view of a Tg(*lhx1a:EGFP;cdh17:mCherry*) larva showing the first *lhx1a:EGFP*$^+$ cell to appear on top of the *cdh17:mCherry*$^+$ embryonic kidney tubules (arrow and inset). **b**, Lateral view of a Tg(*lhx1a:EGFP*) larva showing the extent of *lhx1a:EGFP*$^+$ cell migration (arrows) and their aggregation (arrowheads). **c**, Laser-ablation of an *lhx1a:EGFP*$^+$ aggregate (arrow) inhibits nephron formation without affecting nephrogenesis of an adjacent aggregate (arrowhead). **d**, Time course of a Tg(*lhx1a:EGFP;cdh17:mCherry*) larva demonstrating that *lhx1a:EGFP*$^+$ cells coalesce into an aggregate and differentiate into a nephron. **e**, Time course of a Tg(*wt1b:EGFP;pax8:DsRed*) larva showing development of a *wt1b:EGFP*$^+$ aggregate into a nephron. **f**, Bright field and fluorescent merge of an aggregate from a Tg(*lhx1a:EGFP;cdh17:mCherry*) donor. **g**, Donor-derived *cdh17:mCherry*$^+$ nephrons (one indicated by arrow) and multiple single *lhx1a:EGFP*$^+$ cells (arrowhead) resulting from the transplantation of the aggregate shown in **f** (scale bar, 30 μm). PT, pronephric tubule; sb, swim bladder; larvae shown with anterior to the left.

with stem-cell capabilities, although confirmation of this awaits direct lineage-tracing experiments. Our *in vivo* imaging of nephrogenesis and chimaeric transplantation results demonstrated that nephrogenic aggregates form by the coalescence of multiple *lhx1a:EGFP*$^+$ cells (Supplementary Fig. 1). This process is reminiscent of nephrogenesis in mammals and suggests that similar mechanisms govern nephron formation in both species. Consistent with this, *lhx1a:EGFP*$^+$ cells express *six2a* and *wt1a*, two critical regulators of mammalian nephron progenitors. Our observation that only aggregates of *lhx1a:EGFP*$^+$ cells, but not single cells, are capable of engraftment suggests that nephron progenitor potential may depend upon a 'community effect'[17], a phenomenon whereby continued cell contact is necessary for cells to respond to an inductive signal. The failure of renal vesicles to engraft suggests that nephron-forming potential is lost upon epithelial differentiation.

With our data in hand, it is now possible to pursue whether the mammalian adult kidney contains an equivalent population of nephrogenic aggregates. If present, these cells are most probably dormant or their regenerative abilities blocked, given that nephrogenesis ceases around birth. Using zebrafish to understand the molecular identity of nephron progenitors and the pathways that regulate them may lead to therapeutic ways to activate, or artificially engineer, the mammalian counterpart and augment human renal regeneration. With the rise in chronic kidney disease becoming a serious worldwide healthcare issue, a nephron-progenitor-based regenerative therapy will have a major clinical impact.

METHODS SUMMARY

For WKM transplants, adult recipient fish were conditioned with intraperitoneal injection of gentamicin (80 μg g^{-1}), then immunocompromised with sub-lethal γ-irradiation (25 Gy) to prevent graft rejection[9]. Unpurified WKM cells were prepared as previously described[9] from Tg(*cdh17:EGFP*)[10] or Tg(*cdh17:mCherry*) donors that express fluorescent reporter proteins in the distal nephron. For the *lhx1a:EGFP*$^+$ single cell and aggregate transplants, dissected kidneys from Tg(*lhx1a:EGFP;cdh17:mCherry*) fish were treated with 10% collagenase/dispase for 15 min and cells/aggregates manually transferred with a mouth pipette to a drop of 1X PBS/2% fetal calf serum on a glass slide. A single cell or aggregate was serially passaged through three droplets of PBS/fetal calf serum until free of non-positive cells just before transplantation.

Full Methods and any associated references are available in the online version of the paper at www.nature.com/nature.

Received 19 April; accepted 15 November 2010.
Published online 26 January 2011.

1. Fogo, A. B. Mechanisms of progression of chronic kidney disease. *Pediatr. Nephrol.* **22,** 2011–2022 (2007).
2. Humphreys, B. D. *et al.* Intrinsic epithelial cells repair the kidney after injury. *Cell Stem Cell* **2,** 284–291 (2008).
3. Hartman, H. A., Lai, H. L. & Patterson, L. T. Cessation of renal morphogenesis in mice. *Dev. Biol.* **310,** 379–387 (2007).
4. Reimschuessel, R. A fish model of renal regeneration and development. *ILAR J.* **42,** 285–291 (2001).
5. Zhou, W. *et al.* Characterization of mesonephric development and regeneration using transgenic zebrafish. *Am. J. Physiol. Renal Physiol.* **299,** F1040–F1047 (2010).
6. Wingert, R. A. *et al.* The *cdx* genes and retinoic acid control the positioning and segmentation of the zebrafish pronephros. *PLoS Genet.* **3,** 1922–1938 (2007).
7. Augusto, J., Smith, B., Smith, S., Robertson, J. & Reimschuessel, R. Gentamicin-induced nephrotoxicity and nephroneogenesis in *Oreochromis nilotica*, a tilapian fish. *Dis. Aquat. Organ.* **26,** 49–58 (1996).
8. Kramer-Zucker, A. G., Wiessner, S., Jensen, A. M. & Drummond, I. A. Organization of the pronephric filtration apparatus in zebrafish requires Nephrin, Podocin and the FERM domain protein Mosaic eyes. *Dev. Biol.* **285,** 316–329 (2005).
9. Traver, D. *et al.* Effects of lethal irradiation in zebrafish and rescue by hematopoietic cell transplantation. *Blood* **104,** 1298–1305 (2004).
10. Hall, C. *et al.* Transgenic zebrafish reporter lines reveal conserved Toll-like receptor signaling potential in embryonic myeloid leukocytes and adult immune cell lineages. *J. Leukoc. Biol.* **85,** 751–765 (2009).
11. Kobayashi, A. *et al.* Six2 defines and regulates a multipotent self-renewing nephron progenitor population throughout mammalian kidney development. *Cell Stem Cell* **3,** 169–181 (2008).
12. Purton, L. E. & Scadden, D. T. Limiting factors in murine hematopoietic stem cell assays. *Cell Stem Cell* **1,** 263–270 (2007).
13. Dressler, G. R. The cellular basis of kidney development. *Annu. Rev. Cell Dev. Biol.* **22,** 509–529 (2006).

14. Kobayashi, A. *et al.* Distinct and sequential tissue-specific activities of the LIM-class homeobox gene Lim1 for tubular morphogenesis during kidney development. *Development* **132,** 2809–2823 (2005).
15. Georgas, K. *et al.* Analysis of early nephron patterning reveals a role for distal RV proliferation in fusion to the ureteric tip via a cap mesenchyme-derived connecting segment. *Dev. Biol.* **332,** 273–286 (2009).
16. Swanhart, L. *et al.* Characterization of an *lhx1a* transgenic reporter in zebrafish. *Int. J. Dev. Biol.* **54,** 731–736 (2010).
17. Gurdon, J. B. A community effect in animal development. *Nature* **336,** 772–774 (1988).
18. Lee, Y., Grill, S., Sanchez, A., Murphy-Ryan, M. & Poss, K. D. Fgf signaling instructs position-dependent growth rate during zebrafish fin regeneration. *Development* **132,** 5173–5183 (2005).

Supplementary Information is linked to the online version of the paper at www.nature.com/nature.

Acknowledgements We thank E. C. Liao for help with suturing, and R. Ethier and L. Gyr for zebrafish care. A.J.D. was supported by the Harvard Stem Cell Institute, the American Society of Nephrology and the National Institutes of Health/National Institute of Diabetes and Digestive and Kidney Diseases (P50DK074030).

Author Contributions C.Q.D. and A.J.D. designed the experimental strategy, analysed data, prepared the manuscript, and generated and characterized the Tg(*cdh17:EGFP*), Tg(*cdh17:mCherry*) and Tg(*wt1b:mCherry*) lines. C.Q.D. performed the regeneration, transplants, time course and ablation experiments. C.Q.D., D.M. and R.I.H. made the initial observation that nephron progenitors can be transplanted. N.A.H. generated the Tg(*lhx1a:EGFP*) line (R01DK069403), F.B. and C.E. generated the Tg(*wt1b:EGFP*) line, and T.I. and F.O. provided the Tg(*pax8:DsRed*) line. N.A., R.A.W., G.D. and B.L. analysed kidney expression. H.Z. provided sections of regenerating kidneys. R.C.D., T.M.H., R.W.N., and C.A.C. performed quantitative PCR and microarray analyses. All authors commented on the manuscript.

Author Information Reprints and permissions information is available at www.nature.com/reprints. The authors declare no competing financial interests. Readers are welcome to comment on the online version of this article at www.nature.com/nature. Correspondence and requests for materials should be addressed to A.J.D. (a.davidson@auckland.ac.nz).

METHODS

Zebrafish transgenic lines. Zebrafish were maintained as previously described[19] and according to Institutional Animal Care and Use Committee protocols. The transgenic lines Tg(*wt1b:EGFP*), Tg(*lhx1a:EGFP*) and Tg(*hsp70:dn-fgfr1-EGFP*) were previously reported[16,18,20]. The Tg(*wt1b:mCherry*) line was generated by replacement of EGFP with mCherry in the F47 vector, which contains a shortened version of the *wt1b* promoter that was previously described[20]. The Tg(*cdh17:EGFP*) line was generated by isolation of a 4.3-kb genomic fragment upstream of the Exon 1 5′ untranslated region. The promoter fragment was cloned into the XhoI/SalI sites of the Tol2 vector T2AL200R150G[21]. The Tg(*cdh17:mCherry*) line was generated by co-injection of Cre mRNA with the Tol2 vector T2cdh17-loxP-EGFP-loxP-mCherry. The Tg(*pax8:DsRed*) line was generated by gene trap screening. DsRedExpress was inserted into the BamHI/NotI sites of the pT2KSAG Tol2 vector[22] and was used to generate the transgenic line. Mapping of the insertion site by inverse PCR revealed that DsRedExpress was inserted in the intron region between exons 1 and 2 (T.I. and F.O., unpublished observations).

Adult and larval zebrafish experiments. Epifluorescent images were taken from a Nikon Eclipse 80i microscope using the Hamamatsu ORCA-ER camera and confocal images were acquired using the A1 high-speed confocal Ti-e inverted microscope system (Nikon).

Adult. Gentamicin (40 μg), BrdU (100 μg) and 40 kDa dextran-FITC or -rhodamine (2 μg) were administered by intraperitoneal injection. Single nephrons were dissected in Ringer's buffer using sharpened tungsten needles. Kidney wholemount *in situ* hybridization was as previously described (http://zfin.org/ZFIN/Methods/ThisseProtocol.html) with the addition of 1% dimethyl sulphoxide supplemented to the fixative. Fluorescence-activated cell sorting and analyses were performed using the BD FACSAria (Harvard Stem Cell Institute Flow Cytometry Core Facility). For transplantation of cells directly into the kidney, conditioned recipients were anaesthetized with 0.02% tricaine and a lateral incision was made posterior to the gills and level with the kidney. One microlitre containing approximately 5×10^5 WKM cells, or a single *lhx1a:EGFP*$^+$ cell or a single *lhx1a:EGFP*$^+$ aggregate was injected directly into the head kidney of recipient fish (3 days after conditioning) using a Hamilton syringe. The incision was closed with a suture and the fish was returned to water (Supplementary Fig. 3a–k).

Larva. Larval wholemount *in situ* hybridization was performed as reported[23]. Ablation of *lhx1a:EGFP*$^+$ aggregates was performed with the MicroPoint Laser System (Photonic Instruments) in conjunction with the Nikon Eclipse 80i microscope. For the cellular necrosis assay, water control and gentamicin-treated kidneys were incubated for 10 min in 5 μg ml^{-1} of acridine orange (Sigma) in PBS, washed three times with 50 ml PBS and imaged under bright field and epifluorescence (FITC).

Histology. Haematoxylin and eosin. Kidneys and larvae were fixed in 4% paraformaldehyde, embedded in paraffin, sectioned and stained with haematoxylin and eosin or antibodies against EGFP and BrdU (Dana-Farber/Harvard Cancer Center Pathology Core Facility).

Methylene blue and basic fuchsin. Kidneys were fixed in 4% paraformaldehyde, embedded in JB4 resin, sectioned and stained with methylene blue and basic fuchsin.

Microarray analysis. Triplicate samples of approximately 4,000 *lhx1a:EGFP*$^+$ and *cdh17:EGFP*$^+$ cells were sorted by fluorescence-activated cell sorting into lysis buffer, complementary DNAs were amplified, labelled with Cy3 (*cdh17:EGFP*$^+$) and Cy5 (*lhx1a:EGFP*$^+$), and hybridized to the Agilent Whole Zebrafish Genome Oligo Microarray (3×44k) by Miltenyi Biotec. All statistical analysis used the R package 2.9.2 (http://cran.r-project.org/). Agilent microarrays were processed using the Agilent Feature Extraction software to obtain intensity ratios for each of the 43,803 probes on the array. Intensity ratios from the three separate Agilent microarrays were subsequently quantile normalized using the normalize Between Arrays function in the affy package and differentially expressed gene between cases and controls determined using the limma package. Given the multiple number of hypotheses tested we selected the qvalue package for false discovery rate (FDR) estimation. RMA normalization, limma and qvalue were used to identify differentially expressed probe sets across the eight GUDMAP mouse kidney microarrays of interest (three for *Six2*$^+$ cells, five for proximal tubule cells), which were downloaded from the GEO database (GSE12588, GSE6589 and GSE6290). To compare the differentially expressed genes from the two platforms (and species), the microarray probes were matched to gene identities using annotation files provided by the manufacturers. Zebrafish gene identities were then mapped to mouse orthologues using a combination of the InParanoid (http://inparanoid.sbc.su.se/) and Ensembl databases. A total of 11,870 Ensembl mouse protein identities were identified that could be compared from both arrays. Given the smaller number of zebrafish arrays, FDR thresholds of 40% (nominal $P < 0.016$), 45% ($P < 0.048$) and 50% ($P < 0.11$) were combined with a minimum twofold change in intensity, which corresponded to 1,635, 3,335 and 5,879 probes, respectively. More stringent FDR thresholds of 5% (nominal $P < 0.022$), 10% ($P < 0.07$) and 15% ($P < 0.14$) were chosen for the mouse probes, leading to 5,250, 5,699, 5,936 probe sets, respectively. Genes that were both significantly upregulated and downregulated in the analysis, as judged by separate probes, were excluded, leaving a total of 10,421 genes for comparison. We used Fisher's exact test for statistical significance over a range of FDR values, yielding a range from $P = 0.051$ to $P = 0.86$. The GEO database record number for the zebrafish microarray data is GSE24803.

Quantitative PCR. *lhx1a:EGFP*$^+$ and *cdh17:EGFP*$^+$ cells (300–9,000) were purified by fluorescence-activated cell sorting, lysed and complementary DNA generated using the Cells-to-cDNA kit (Ambion). Quantitative PCR was performed in triplicate using SYBR Green chemistry on a Mastercycler RealPlex^2 PCR machine (Eppendorf) using the following primer sets: *slc20a1a* forward 5′-TCTCTG GGACACATTGCATC-3′, reverse 5′-AGCAGTTCCAGCCATTTGAC-3′; *slc13a1* forward 5′-TGCTGGGATTCCTGTTCTTC-3′, reverse 5′-AAACCTCCACCAA CAAGCAG-3′; *slc12a1* forward 5′-TCAACGCTCTGAAGAAGCTG-3′, reverse 5′-ACGTTGTGTGGGTTTCTTCC-3′; *slc12a3* forward 5′-ACAGATCCGGCTG AATGAAG-3′, reverse 5′-AGCCAAGCCATGTAAAGAGG-3′; *six2a* forward 5′-AGCTCGGAGGATGAGTTTTC-3′, reverse 5′-ATGGTGCCTTGCAGAAG AAG-3′; *wt1a* forward 5′-AGCCAACCAAGGATGTTCAG-3′, reverse 5′-AACC TTGATTCCTGGAGCTG-3′. *ef1a* was used as the normalization control: forward 5′-CTGGAGGCCAGCTCAAACAT-3′, reverse 5′-ATCAAGAAGAGTAGTAC CGCTAGCATTAC-3′. Relative quantification of target gene expression was evaluated using the comparative C_T method. A mean and standard deviation were determined for the ΔC_T value for all genes of interest. The error in fold-change was obtained by considering the effect of an increase or decrease of one standard deviation in ΔC_T value.

19. Westerfield, M. *The Zebrafish Book: A Guide for the Laboratory Use of Zebrafish* (Danio rerio) 4th edn (Univ. Oregon Press, 2000).
20. Perner, B., Englert, C. & Bollig, F. The Wilms tumor genes *wt1a* and *wt1b* control different steps during formation of the zebrafish pronephros. *Dev. Biol.* **309,** 87–96 (2007).
21. Urasaki, A., Morvan, G. & Kawakami, K. Functional dissection of the tol2 transposable element identified the minimal *cis*-sequence and a highly repetitive sequence in the subterminal region essential for transposition. *Genetics* **174,** 639–649 (2006).
22. Kawakami, K. *et al.* A transposon-mediated gene trap approach identifies developmentally regulated genes in zebrafish. *Dev. Cell* **7,** 133–144 (2004).
23. Elizondo, M. R. *et al.* Defective skeletogenesis with kidney stone formation in dwarf zebrafish mutant for *trpm7*. *Curr. Biol.* **15,** 667–671 (2005).